23
Quasielastic scattering

A first description of quasielastic scattering is obtained from the electromagnetic response of a non-interacting, non-relativistic Fermi gas. This provides a convenient, consistent picture of the dominant part of the nuclear response surface as a function of $(\mathbf{q}, \omega)$. Consider a Fermi gas of protons as illustrated in Fig. 23.1. The total charge and charge density are obtained by counting the occupied states

$$\begin{aligned} Z &= \sum_{\mathbf{k}\lambda}^{k_F} 1 \to \frac{2\Omega}{(2\pi)^3} \int_0^{k_F} d^3k = \frac{\Omega k_F^3}{3\pi^2} \\ \frac{Z}{\Omega} &\equiv \rho = \frac{k_F^3}{3\pi^2} \end{aligned} \tag{23.1}$$

The last equality relates the proton density to the Fermi wave number. For illustration, retain just the Coulomb interaction, assuming no transverse interaction. The target response surfaces of chapter 11 then reduce to the form [compare Eq. (12.31)]

$$\begin{aligned} W_1 &= 0 \\ \frac{1}{M_T} W_2 &= \frac{q_\mu^4}{\mathbf{q}^4} \overline{\sum_i} \sum_f |\langle f| \int \exp(-i\mathbf{q}\cdot\mathbf{x})\, \hat{\rho}(\mathbf{x})\, d^3x |i\rangle|^2 \delta(W_f - W_i) \end{aligned} \tag{23.2}$$

The notation used is indicated in Fig. 23.2.[1]

[1] Use of translational invariance, with eigenstates of three-momentum, allows one to do both spatial integrations which yield, in the limit of large Ω, a factor $(2\pi)^3 \Omega \delta^{(3)}(\mathbf{P}_f - \mathbf{P}_i)$ — this reproduces the previous form for the response surfaces for a target initially at rest. In the present form, one can directly calculate the scattering for a stationary target.

https://doi.org/10.1017/9781009290616.028 Published online by Cambridge University Press

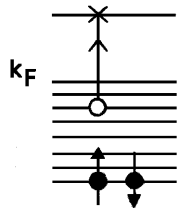

Fig. 23.1. Response of Fermi gas.

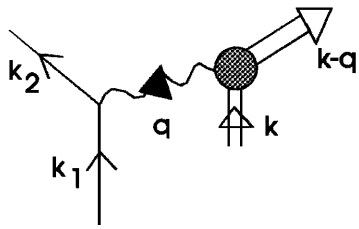

Fig. 23.2. Notation in calculation of Coulomb response of Fermi gas.

We also extract the nucleon form factor of Eq. (19.22) and write

$$\frac{1}{M_T} W_2 \equiv \frac{q_\mu^4}{\mathbf{q}^4} |f_{\mathrm{SN}}(q^2)|^2 R(\mathbf{q}^2, \omega) \tag{23.3}$$

Here $\omega \equiv \varepsilon_1 - \varepsilon_2$ is the energy loss.

The charge density operator for point protons can then be written in second quantization as

$$\hat{\rho}(\mathbf{x}) = \hat{\psi}^\dagger(\mathbf{x})\hat{\psi}(\mathbf{x}) \tag{23.4}$$

Here, the non-relativistic, two-component proton field is given by

$$\hat{\psi}(\mathbf{x}) = \frac{1}{\sqrt{\Omega}} \sum_{\mathbf{k}\lambda} a_{\mathbf{k}\lambda} \exp(i\mathbf{k} \cdot \mathbf{x})\, \eta_\lambda \tag{23.5}$$

Thus, upon integration

$$\int \exp(-i\mathbf{q} \cdot \mathbf{x})\, \hat{\rho}(\mathbf{x})\, d^3x = \sum_{\mathbf{k}\lambda} a^\dagger_{\mathbf{k}-\mathbf{q},\lambda} a_{\mathbf{k}\lambda} \tag{23.6}$$

Matrix elements of this expression for a Fermi gas can now be readily evaluated. One particle must be destroyed inside the Fermi sea and one created outside. Upon converting the final sum to an integral, one arrives at

$$R(\mathbf{q}^2, \omega) = \frac{2\Omega}{(2\pi)^3} \int_0^{k_F} d^3k\, \theta(|\mathbf{k} - \mathbf{q}| - k_F)\delta(\omega - \varepsilon_{\mathbf{k}-\mathbf{q}} + \varepsilon_{\mathbf{k}}) \tag{23.7}$$

https://doi.org/10.1017/9781009290616.028 Published online by Cambridge University Press

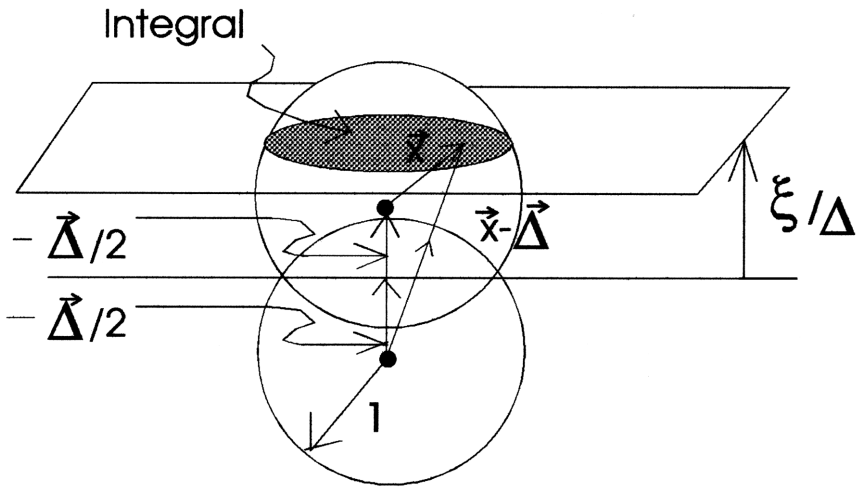

Fig. 23.3. Momentum space geometry for evaluation of response of a non-relativistic Fermi gas.

This is a general result for a Fermi gas. Now specialize to the dispersion relation for non-relativistic nucleons

$$\begin{aligned} \varepsilon_{\mathbf{k}} &= \frac{\mathbf{k}^2}{2m} \\ R(\mathbf{q}^2,\omega) &= \frac{2\Omega}{(2\pi)^3}\int_0^{k_F} d^3k\,\theta(|\mathbf{k}-\mathbf{q}|-k_F)\,\delta\left(\omega+\frac{\mathbf{k}\cdot\mathbf{q}}{m}-\frac{\mathbf{q}^2}{2m}\right) \end{aligned} \tag{23.8}$$

Introduce dimensionless variables according to

$$\mathbf{x}\equiv\frac{\mathbf{k}}{k_F} \qquad ;\ \Delta\equiv\frac{\mathbf{q}}{k_F} \qquad ;\ \xi\equiv\frac{m\omega}{k_F^2} \tag{23.9}$$

The additional use of $\Omega = 3\pi^2 Z/k_F^3$ then leads to

$$R(\mathbf{q}^2,\omega)=\frac{3Z}{4\pi}\frac{m}{k_F^2}\int_0^1 d^3x\,\theta(|\mathbf{x}-\mathbf{\Delta}|-1)\,\delta\left(\xi+\mathbf{\Delta}\cdot\mathbf{x}-\frac{\mathbf{\Delta}^2}{2}\right) \tag{23.10}$$

This integral can be done with the aid of some simple geometric considerations [Fe71]. The situation is illustrated in Fig. 23.3. First rewrite

$$\delta\left(\xi+\mathbf{\Delta}\cdot\mathbf{x}-\frac{\mathbf{\Delta}^2}{2}\right)=\frac{1}{\Delta}\delta\left(\mathbf{x}\cdot\left[\frac{\mathbf{\Delta}}{\Delta}\right]+\frac{\xi}{\Delta}-\frac{\Delta}{2}\right) \tag{23.11}$$

Energy conservation enforced by the vanishing of the argument of the

https://doi.org/10.1017/9781009290616.028 Published online by Cambridge University Press

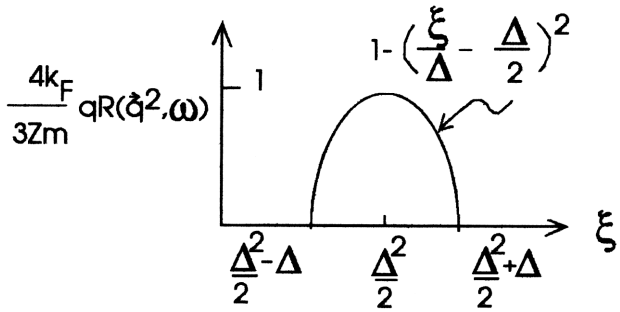

Fig. 23.4. The quantity $\zeta R(\mathbf{q}^2, \omega)$ with $\zeta \equiv 4k_F q/3Zm$ for the case $\Delta \geq 2$.

delta function then defines the plane indicated in this figure

$$-\mathbf{x} \cdot \left[\frac{\mathbf{\Delta}}{\Delta}\right] = \frac{\xi}{\Delta} - \frac{\Delta}{2} \tag{23.12}$$

The restrictions on the region of integration reflect the fact that the particle is initially inside the Fermi sphere (F) and must end up outside

$$\begin{aligned} |\mathbf{x} - \mathbf{\Delta}| &> 1 \qquad ; \text{ outside F} \\ |\mathbf{x}| &\leq 1 \qquad ; \text{ inside F} \end{aligned} \tag{23.13}$$

The answer for the $\Delta \times$ (integral) is the area of intersection of the plane and the restricted Fermi sphere. This is either a circle (as illustrated in the figure), or an annulus, depending on the value of ξ/Δ. Thus one can immediately write the answer in the various cases:

1) $\Delta \geq 2$ (spheres do not intersect)

$$\begin{aligned} \frac{\Delta}{2} + 1 &\geq \frac{\xi}{\Delta} \geq \frac{\Delta}{2} - 1 \qquad ; \text{ plane intersects sphere} \\ \text{area} &= \pi \left[1^2 - \left(\frac{\xi}{\Delta} - \frac{\Delta}{2}\right)^2\right] \\ R(\mathbf{q}^2, \omega) &= \frac{3Z}{4\pi} \frac{m}{k_F^2} \frac{\pi}{\Delta} \left[1^2 - \left(\frac{\xi}{\Delta} - \frac{\Delta}{2}\right)^2\right] \end{aligned} \tag{23.14}$$

This result is sketched in Fig. 23.4, and we make two observations:

- The peak of this response occurs at $\xi = \Delta^2/2$ or

$$\omega_{\text{peak}} = \mathbf{q}^2/2m \tag{23.15}$$

This is just the free, non-relativistic kinematic relation for the energy transfer to a nucleon initially at rest, recoiling with momentum $-\mathbf{q}$. Note the position of this quaiselastic peak moves with $\mathbf{q}^2$.

https://doi.org/10.1017/9781009290616.028 Published online by Cambridge University Press

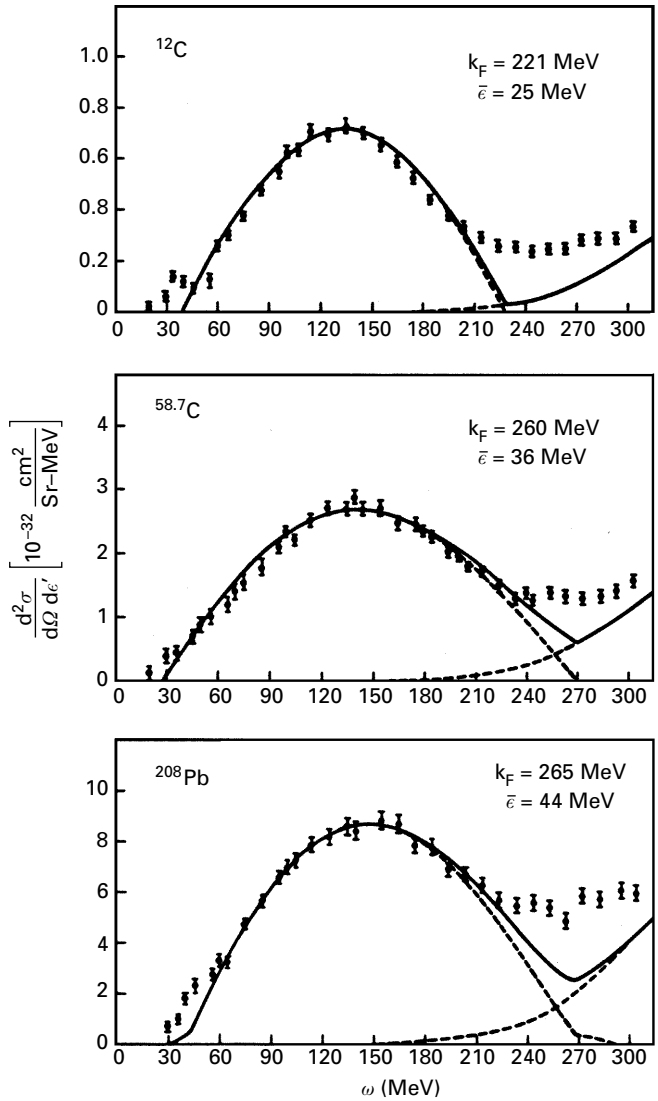

Fig. 23.5. Data on quasielastic scattering at $\varepsilon_1 = 500\,\text{MeV}, \theta = 60^\circ$ from HEPL. Calculation includes Coulomb and transverse current interactions. $\bar{\varepsilon}$ shifts the response function by an average nuclear binding energy [Mo71, Do75].

- The width of this peak at the base is 2Δ. Thus $\delta\xi_{\text{base}} = 2\Delta$ or

$$\frac{1}{2}\delta\omega_{\text{base}} = \frac{k_F}{m}|\mathbf{q}| = v_F|\mathbf{q}| \tag{23.16}$$

There is a Doppler broadening of the quasielastic peak that increases with $|\mathbf{q}|$. This width can be used to measure the Fermi velocity as shown in Fig. 23.5.

https://doi.org/10.1017/9781009290616.028 Published online by Cambridge University Press

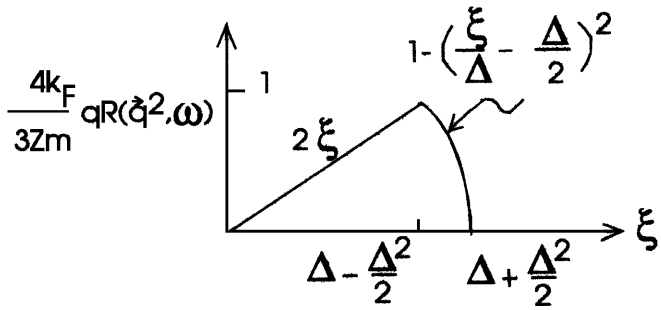

Fig. 23.6. The quantity $\zeta R(\mathbf{q}^2,\omega)$ with $\zeta \equiv 4k_F q/3Zm$ for the case $\Delta \leq 2$.

2) $\Delta \leq 2$ (spheres intersect)

$$\begin{aligned} 1+\frac{\Delta}{2} &\geq \frac{\xi}{\Delta} \geq 1-\frac{\Delta}{2} \quad \text{; plane does not intersect excluded sphere} \\ R(\mathbf{q}^2,\omega) &= \frac{3Z}{4\pi}\frac{m}{k_F^2}\frac{\pi}{\Delta}\left[1^2-\left(\frac{\xi}{\Delta}-\frac{\Delta}{2}\right)^2\right] \end{aligned} \tag{23.17}$$

The area and answer are the same as before.

3) $\Delta \leq 2$ (spheres intersect)

$$\begin{aligned} 1-\frac{\Delta}{2} &\geq \frac{\xi}{\Delta} \geq 0 \qquad\qquad \text{; plane does intersect excluded sphere} \\ \text{area} &= \pi\left\{\left[1^2-\left(\frac{\xi}{\Delta}-\frac{\Delta}{2}\right)^2\right]-\left[1^2-\left(\frac{\xi}{\Delta}+\frac{\Delta}{2}\right)^2\right]\right\} = 2\pi\xi \\ R(\mathbf{q}^2,\omega) &= \frac{3Z}{4\pi}\frac{m}{k_F^2}2\pi\left(\frac{\xi}{\Delta}\right) \end{aligned} \tag{23.18}$$

The results in the case $\Delta \leq 2$ are sketched in Fig. 23.6.

This simple model calculation provides excellent insight into quasielastic electron scattering from the nuclear many-body system.

Within the traditional framework of non-relativistic nucleons and one-body densities, it is possible to derive some *exact* results for the nuclear response functions. An integration over all energy loss in Eq. (23.2) at fixed $\mathbf{q}$ removes the energy delta function, and from Eqs. (23.3) and (23.4)[2]

$$S(\mathbf{q}^2) \equiv \int d\omega R(\mathbf{q}^2,\omega) = \sum_f |\langle\Psi_f| \int \exp(-i\mathbf{q}\cdot\mathbf{x})\,\hat{\rho}(\mathbf{x})\,d^3x|\Psi_0\rangle|^2 \tag{23.19}$$

[2] It is important to note that one can never fully evaluate this integral experimentally in electron scattering since there the four-momentum transfer must be space-like $q_\mu^2 = \mathbf{q}^2-\omega^2 \geq 0$.

https://doi.org/10.1017/9781009290616.028 Published online by Cambridge University Press

Here the ground state is written as $|i\rangle \equiv |\Psi_0\rangle$; it is assumed to be non-degenerate. Closure may now be used on this expression to give

$$S(\mathbf{q}^2) = \langle\Psi_0| \int\int d^3x\, d^3y \exp\{-i\mathbf{q}\cdot(\mathbf{x}-\mathbf{y})\}\, \hat{\rho}(\mathbf{y})\, \hat{\rho}(\mathbf{x})\, |\Psi_0\rangle \tag{23.20}$$

Now make use of the canonical anti-commutation rules for the proton fields

$$\begin{aligned} \left\{\hat{\psi}_\alpha(\mathbf{x}),\, \hat{\psi}^\dagger_\beta(\mathbf{y})\right\} &= \delta^{(3)}(\mathbf{x}-\mathbf{y})\, \delta_{\alpha\beta} \\ \{\hat{\psi}_\alpha(\mathbf{x}),\, \hat{\psi}_\beta(\mathbf{y})\} &= \left\{\hat{\psi}^\dagger_\alpha(\mathbf{x}),\, \hat{\psi}^\dagger_\beta(\mathbf{y})\right\} = 0 \end{aligned} \tag{23.21}$$

They allow one to write

$$\begin{aligned} \hat{\rho}(\mathbf{y})\, \hat{\rho}(\mathbf{x}) &= \hat{\psi}^\dagger(\mathbf{y})\hat{\psi}(\mathbf{y})\hat{\psi}^\dagger(\mathbf{x})\hat{\psi}(\mathbf{x}) \\ &= \delta^{(3)}(\mathbf{x}-\mathbf{y})\hat{\psi}^\dagger(\mathbf{x})\hat{\psi}(\mathbf{x}) + \hat{\psi}^\dagger(\mathbf{y})\hat{\psi}^\dagger(\mathbf{x})\hat{\psi}(\mathbf{x})\hat{\psi}(\mathbf{y}) \end{aligned} \tag{23.22}$$

The total charge, a constant of the motion, can be identified according to

$$\int d^3x \int d^3y \exp\{-i\mathbf{q}\cdot(\mathbf{x}-\mathbf{y})\}\, \delta^{(3)}(\mathbf{x}-\mathbf{y})\, \hat{\psi}^\dagger(\mathbf{x})\, \hat{\psi}(\mathbf{x}) = \hat{Z} \tag{23.23}$$

Hence one has the general result

$$\begin{aligned} S(\mathbf{q}^2) &= Z \\ &+ \int d^3x \int d^3y\, \exp\{-i\mathbf{q}\cdot(\mathbf{x}-\mathbf{y})\}\, \langle\Psi_0|\hat{\psi}^\dagger(\mathbf{y})\hat{\psi}^\dagger(\mathbf{x})\hat{\psi}(\mathbf{x})\hat{\psi}(\mathbf{y})|\Psi_0\rangle \end{aligned} \tag{23.24}$$

The discussion can be focused on inelastic transitions by defining S^{in} through the restriction $\sum_{f\neq 0}$ in Eq. (23.19). This yields

$$S^{\text{in}}(\mathbf{q}^2) = S(\mathbf{q}^2) - |\langle\Psi_0| \int \exp(-i\mathbf{q}\cdot\mathbf{x})\, \hat{\rho}(\mathbf{x})\, d^3x\, |\Psi_0\rangle|^2 \tag{23.25}$$

It follows that

$$\begin{aligned} S^{\text{in}}(\mathbf{q}^2) &\equiv \int d\omega\, R^{\text{in}}(\mathbf{q}^2, \omega) \\ &= Z + \int\int d^3x\, d^3y\, \exp\{-i\mathbf{q}\cdot(\mathbf{x}-\mathbf{y})\}\, g(\mathbf{x},\mathbf{y}) \\ g(\mathbf{x},\mathbf{y}) &\equiv \langle\Psi_0|\hat{\psi}^\dagger(\mathbf{y})\hat{\psi}^\dagger(\mathbf{x})\hat{\psi}(\mathbf{x})\hat{\psi}(\mathbf{y})|\Psi_0\rangle \\ &\quad -\langle\Psi_0|\hat{\psi}^\dagger(\mathbf{x})\hat{\psi}(\mathbf{x})|\Psi_0\rangle\langle\Psi_0|\hat{\psi}^\dagger(\mathbf{y})\hat{\psi}(\mathbf{y})|\Psi_0\rangle \end{aligned} \tag{23.26}$$

One observes that $g(\mathbf{x},\mathbf{y})$ in the nuclear two-body charge density, and this Coulomb sum rule provides probably the only way, in principle, to unambiguously measure this *density–density correlation function* in nuclei. If the Fourier transform of the two-body density goes to zero as $|\mathbf{q}| \to \infty$, then

$$S^{\text{in}}(\mathbf{q}^2) \to Z \qquad ;\ |\mathbf{q}| \to \infty \tag{23.27}$$

https://doi.org/10.1017/9781009290616.028 Published online by Cambridge University Press

In this limit, in this traditional picture, the Coulomb sum rule simply counts the number of proton charges.

The Coulomb sum rule can be explicitly evaluated for a Fermi gas by integrating the previously derived response functions. First note that $d\xi = m\,d\omega/k_F^2$, and define $y \equiv \xi/\Delta$. Then

1) For $\Delta \geq 2$

$$S^{\rm in}(\mathbf{q}^2) = \frac{3Z}{4}\int_{\Delta/2-1}^{\Delta/2+1} dy\left[1-\left(y-\frac{\Delta}{2}\right)^2\right] \tag{23.28}$$

Change variables to $u \equiv y - \Delta/2$ and use $\int_{-1}^{1} du(1-u^2) = 4/3$, thus

$$S^{\rm in}(\mathbf{q}^2) = Z \tag{23.29}$$

2) For $\Delta \leq 2$

$$\begin{aligned} S^{\rm in}(\mathbf{q}^2) &= \frac{3Z}{4}\left\{\int_0^{1-\Delta/2} 2\Delta\, y\, dy + \int_{1-\Delta/2}^{1+\Delta/2} dy\left[1-\left(y-\frac{\Delta}{2}\right)^2\right]\right\} \\ &= \frac{3Z}{4}\left[2\Delta\frac{1}{2}\left(1-\frac{\Delta}{2}\right)^2 + \int_{1-\Delta}^{1} du(1-u^2)\right] \\ &= \frac{3Z}{4}\left(\Delta - \frac{1}{12}\Delta^3\right) \end{aligned} \tag{23.30}$$

Thus

$$S^{\rm in}(\mathbf{q}^2) = Z\left(\frac{3}{4}\Delta - \frac{1}{16}\Delta^3\right) \tag{23.31}$$

In *summary*, the Coulomb sum rule defined by

$$C^{\rm in}(q) \equiv \frac{1}{Z}S^{\rm in}(q) \tag{23.32}$$

takes the following form for a non-relativistic Fermi gas

$$\begin{aligned} C^{\rm in}(q) &= 1 && ;\ q \geq 2k_F \\ &= \frac{3}{2}\left(\frac{q}{2k_F}\right) - \frac{1}{2}\left(\frac{q}{2k_F}\right)^3 && ;\ q \leq 2k_F \end{aligned} \tag{23.33}$$

This result is plotted as $C(Q)_{\rm NR}$ in Fig. 23.7.[3]

[3] In the quantum field theory QHD-I, described by the lagrangian density of Eq. (21.1), the baryon field satisfies canonical anti-commutation relations; however, it contains both baryons and anti-baryons. The equations of motion imply that the local, effective current in Eq. (21.14) is conserved. A Coulomb sum rule can then be constructed in direct analogy with the derivation given in the text. The result obtained for nuclear

https://doi.org/10.1017/9781009290616.028 Published online by Cambridge University Press

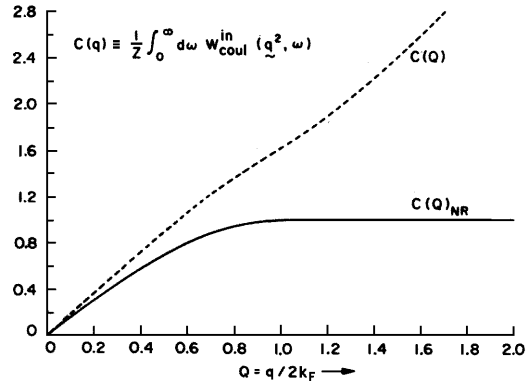

Fig. 23.7. The Coulomb sum rule $C(Q)$ where $Q = q/2k_F$. The non-relativistic result (NR) is that of Eq. (23.33). Also shown is the RMFT result (see text).

Inspection of Eqs. (23.3) and (23.8) shows that in the non-interacting, non-relativistic Fermi gas, the Coulomb cross section can be written

$$\begin{aligned} \frac{d^2\sigma}{d\varepsilon_2 d\Omega_2} &= \sigma_M \frac{q_\mu^4}{\mathbf{q}^4} |f_{\rm SN}(q^2)|^2 R(\mathbf{q}^2, \omega) \\ R(\mathbf{q}^2, \omega) &= \frac{3Z}{4\pi k_F^3} \int_0^{k_F} d^3k\, \theta(|\mathbf{k}-\mathbf{q}| - k_F)\delta(\omega + \frac{\mathbf{k}\cdot\mathbf{q}}{m} - \frac{\mathbf{q}^2}{2m}) \end{aligned} \tag{23.34}$$

Here we have used $\Omega = 3\pi^2 Z/k_F^3$. Now write the momentum integration region in Eq. (23.34) as $d^2k_\perp dk_\parallel$ where $\mathbf{k}_\parallel$ lies along $\mathbf{q}$, and assume that the momentum transfer $\mathbf{q}$ is large enough so that the θ function in the integrand is irrelevant. Then

$$\begin{aligned} \frac{d^2\sigma}{d\varepsilon_2 d\Omega_2} &= \sigma_M \frac{q_\mu^4}{\mathbf{q}^4} |f_{\rm SN}(q^2)|^2 \frac{m}{q} F(y) \qquad ; \mathbf{q} \to \infty \\ F(y) &= \frac{3Z}{4\pi k_F^3} \int_0^{k_F} d^2k_\perp\, dk_\parallel\, \delta(k_\parallel - y) \\ y &\equiv \frac{m\omega}{q} - \frac{q}{2} \end{aligned} \tag{23.35}$$

The energy loss ω and momentum transfer $q \equiv |\mathbf{q}|$ enter the *scaling function* $F(y)$ only through the single *scaling variable* y.

---

matter, using RMFT to evaluate the two-body charge density, is shown in Fig. 23.7 [Wa83]. The Coulomb response amplitudes are more complicated in a full field theory. For example, there are other degrees of freedom that carry charge, included here in an empirical fashion in the additional anomalous magnetic moment term in the effective current [responsible for the rise in $C(\mathbf{q}^2)$]. It is also possible to produce real nucleon pairs in the time-like region [Ma83]. The nuclear Coulomb sum rule in such theories is examined in detail in [Fe94, Ko95].

https://doi.org/10.1017/9781009290616.028 Published online by Cambridge University Press

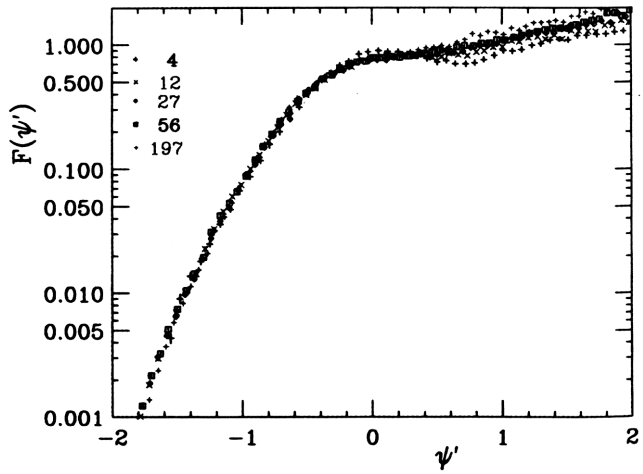

Fig. 23.8. Super-scaling analysis of Donnelly and Sick for nuclei from $A = 4$–197 [Do99]. The variable ψ', defined in that paper, is close to y/k_F.

Suppose one still has a non-interacting, non-relativistic Fermi gas but now, instead of the initial momentum distribution $(3/4\pi k_F^3)\theta(k_F - k)$, one has a more general (normalized) distribution $n(\mathbf{k}^2)$. One example would be a *thermal* Fermi distribution [Fe71]. Suppose also that the Pauli Principle is irrelevant for the final-state proton. The evident generalization of Eq. (23.35) is

$$\begin{aligned} F(y) &= \int d^2k_\perp\, dk_\parallel\, n(\mathbf{k}_\perp^2 + \mathbf{k}_\parallel^2)\, \delta(k_\parallel - y) \\ &= \int d^2k_\perp\, n(\mathbf{k}_\perp^2 + y^2) \\ y &\equiv \frac{m\omega}{q} - \frac{q}{2} \end{aligned} \tag{23.36}$$

This result is known as *y-scaling*. It is a simple result of conservation of energy and momentum for a non-relativistic nucleon. To the extent that the nuclear density and Fermi momentum are unchanged as the size of the nucleus is increased, $F(y)$ should be a universal function independent of A. y-scaling is discussed in detail in the review article [Da90]. One of the most impressive applications of y-scaling is in the work of Donnelly and Sick shown in Fig. 23.8 [Do99], which reflects some of the extended relativistic analysis in appendix G.

The response of the relativistic Fermi gas is investigated in depth in [Mo69, Va78, Al88, Ce97]. Smith and Moniz [Sm72] have also calculated inclusive quaiselastic scattering $(\mathrm{e}, \mathrm{e}')$ in a relativistic Fermi gas model of

https://doi.org/10.1017/9781009290616.028 Published online by Cambridge University Press

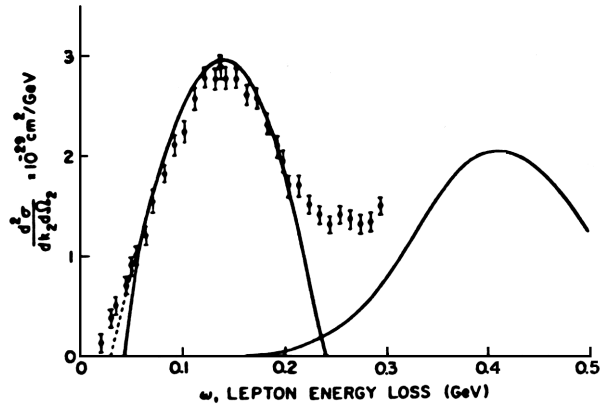

Fig. 23.9. Relativistic calculation of quasielastic peak and $N^\star(1232)$ production in electron scattering from Ni at $\varepsilon_1 = 500\,\text{MeV}$, and $\theta = 60^\circ$; here $\bar{\varepsilon} = 42\,\text{MeV}$ and $k_F = 271\,\text{MeV}$ [Sm72]. The experimental data are from Moniz *et al.* [Mo71]. The dashed line omits the Pauli principle in the final state.

the nucleus, including production of the $\Delta(1232)$ (see chapter 28). Their results for Ni are shown in Fig. 23.9.

A relativistic model which includes interactions in an average fashion is given by relativistic mean field theory (RMFT) discussed in chapter 21. Pollock has calculated the four response functions of Eq. (13.48) for coincident electron scattering (e, e′ N) for nuclear matter in RMFT [Po88]. He uses the current of Eq. (21.14), and his results are shown in Fig. 23.10. This is a very simple calculation, but it has the following features to recommend it:

- The RMFT provides a realistic model of nuclear matter [Wa95];
- The full nucleon vertex $\Gamma_\mu = F_1\gamma_\mu - F_2\sigma_{\mu\nu}k_\nu$ has been used; the current is conserved and gives the correct result for a free nucleon;
- The calculation is completely relativistic;
- The resulting response surfaces in Fig. 23.10 map out the complete Fermi sphere, weighted with the appropriate electromagnetic interaction; one can examine any part of the Fermi sphere, including the deeply bound states, by looking at the appropriate region of the response surface. Correlations will modify the Fermi sphere and add a tail to the momentum distribution;
- The (e, e′ n) surfaces are also worth looking at [Po88].

Figures 21.2 and 21.3 show quasielastic data from HEPL on $^{40}_{20}$Ca(e, e′)

https://doi.org/10.1017/9781009290616.028 Published online by Cambridge University Press

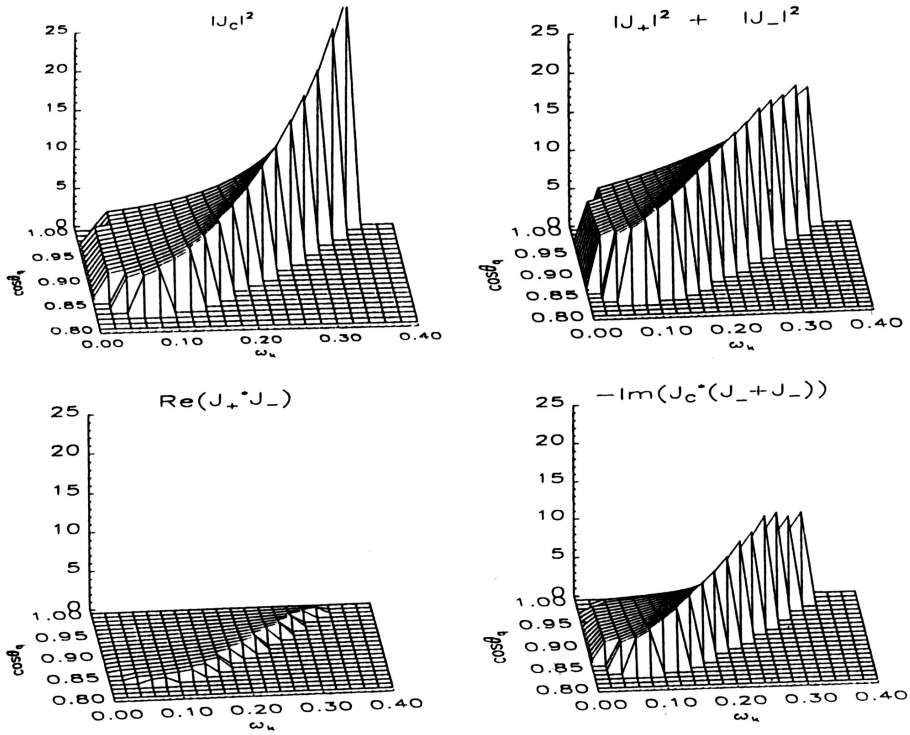

Fig. 23.10. The four proton response functions in RMFT obtained from the transition matrix elements of the current $\mathscr{J}_\mu$ and evaluated per proton are plotted as functions of energy loss and $\cos\theta_q$. Here $|\mathbf{k}| = 0.5\,\text{GeV}$ and $\phi_q = \pi/2$; the ϕ_q dependence is now in the response. Also $k_F = 0.28\,\text{GeV}$ and $m^\star/m = 0.56$ (appropriate for nuclear matter). The vertical scale is $25.0\,\text{GeV}^{-1}$ for all four response functions, and ω_k is in GeV [Po88, Wa95].

and ${}^{208}_{82}\text{Pb}(\text{e},\text{e}')$ compared with a calculation in RMFT [Ro80].[4] The calculation uses the relativistic densities for these nuclei, and the full, relativistic, conserved current; there are no free parameters. The position, shape, and magnitude of the peak are all well-described; it would appear that one had an understanding of nuclear quasielastic scattering. Nonetheless, the data contains both the transverse and Coulomb (longitudinal) response, and if one could isolate the Coulomb response, where the interaction is simply with the charges in the target, the understanding should be even better. Experimentalists have worked very hard to make the required Rosenbluth separation, and the result for ${}^{40}_{20}\text{Ca}$ is shown in Fig. 23.11. The experimental points are from Saclay; they represent the area under the Coulomb

[4] Quasielastic electron scattering for ${}^{40}_{20}\text{Ca}(\text{e},\text{e}')$ is calculated in relativistic Hartree by summing over single-particle transitions, and including the RPA response, in [Ho89].

https://doi.org/10.1017/9781009290616.028 Published online by Cambridge University Press

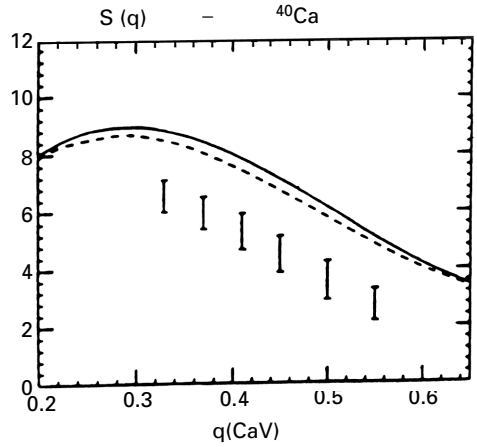

Fig. 23.11. Area under the Coulomb part of the quasielastic peak — the Coulomb sum rule — for $^{40}_{20}$Ca(e, e′). Data are from Saclay [Me84]. Theoretical curve is RMFT, with relativistic, conserved current and nucleon form factors left in [Po88, Wa95].

quasielastic peak — the Coulomb sum rule. The theoretical curve is the same RMFT calculation described above [Po88].[5] The disagreement is by almost a factor of 2 at the largest q. Several possible solutions have been proposed, including: a swelling of the nucleon in the nuclear medium [now pretty well ruled out by further (e, e′) studies], modification of strong, hadronic vacuum polarization in the nuclear medium, RPA correlations, short-range correlations, and missing experimental strength.

Consider further one of these effects, the role of short-range correlations in the Coulomb sum rule. Recall from Eqs. (23.26) and (23.32) that the Coulomb sum rule, properly normalized[6] can be written [Vi77, Wa93]

$$C^{\text{in}}(q) = 1 + \tilde{\rho}^{(2)}_{pp}(q) \tag{23.37}$$

The second term is the Fourier transform of the two-body density. Figure 23.12 [Vi77] shows the calculated quantity $|1 - C^{\text{in}}(q)|$ for infinite nuclear matter using (1) The Pauli correlations of a non-interacting Fermi gas; (2) A two-body density calculated from the Bethe–Goldstone wave function for a hard-core interaction [Fe71]; (3) A similar result with a more realistic two-body interaction. While approximately 10% correction from short-range correlations at the highest measured q above is conceivable; it is difficult to see how this could account for the factor of 2.

[5] The single-nucleon form factors have been left in this result.

[6] The normalization is $C^{\text{in}}(q) \to 0$ as $q \to 0$, and the single-nucleon form factor has been divided out.

https://doi.org/10.1017/9781009290616.028 Published online by Cambridge University Press

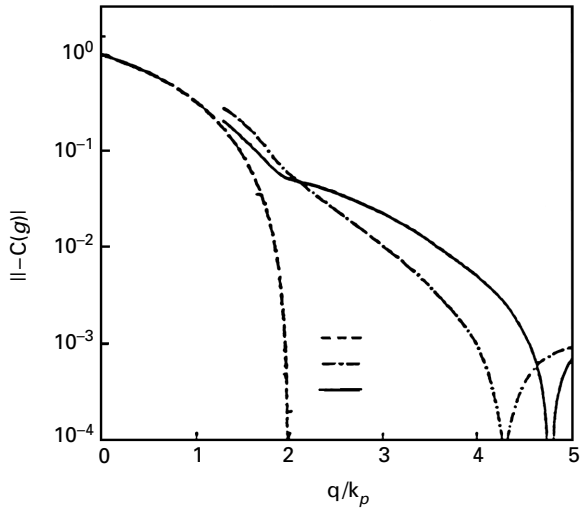

Fig. 23.12. Normalized Coulomb sum rule for nuclear matter including short-range correlations (see text) [Vi77] .

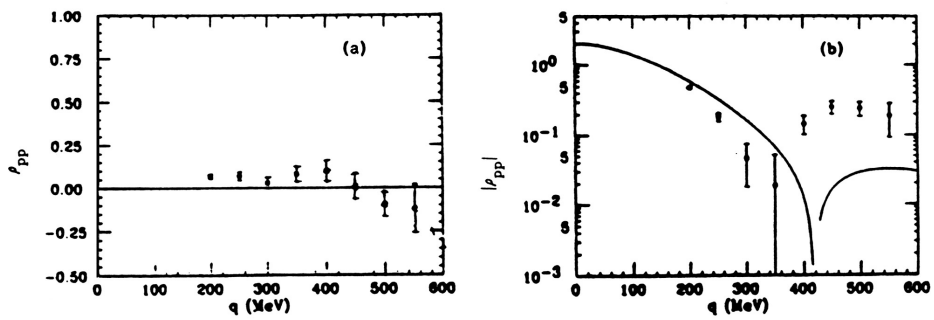

Fig. 23.13. Two-body density $\tilde{\rho}^{(2)}_{pp}(q)$ extracted from Coulomb sum rule in (a) ${}^3_1\mathrm{H(e,e')}$ and (b) ${}^3_2\mathrm{He(e,e')}$. The data are from Bates [Be90].

The two-body density is one of the fundamental quantities in many-particle physics. For example, the precision measurement of this quantity by inelastic neutron scattering in liquid ^{4}He provides the basis for much of our understanding of this quantum fluid. Despite the fact that the two-body density is the basic quantity used in the calculation of the binding energy of many-body nuclei, it had never been measured experimentally. It *has* now been measured, however, for one simple system.

A study of quasielastic scattering in both ${}^3_2\mathrm{He(e,e')}$ and ${}^3_1\mathrm{H(e,e')}$ has been carried out at Bates. Figure 23.13 shows the two-body density extracted from the Coulomb sum rule in these two nuclei [Be90]. This determination has a very nice self-calibration, for the two-body proton

https://doi.org/10.1017/9781009290616.028 Published online by Cambridge University Press

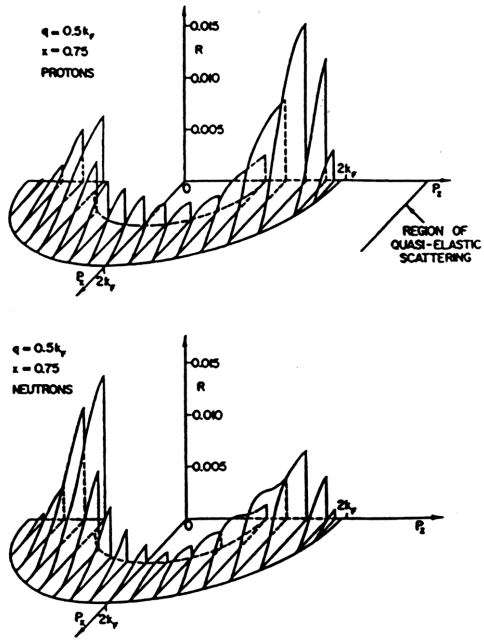

Fig. 23.14. Nuclear Coulomb response (dimensionless units) for n.m.(e, e′ N) for hard-core Fermi gas to order $(k_F a)^2$. x is dimensionless energy transfer. Kinematics arranged so there is no quasi-elastic (e, e′ p) [de66a, de67, Wa93].

density must *vanish* in ${}^3_1$H, as it does. The result for ${}^3_2$He provides the first experimental determination of the two-body nuclear density — a significant achievement.

The resolution of the disagreement with the Coulomb sum rule in medium to heavy nuclei has been one of the most significant problems in nuclear physics [Wa95]. Jourdan has made a very important contribution here [Jo96]. By combining all the available data from the world's laboratories, he shows that it is possible to obtain a longer lever arm on the Rosenbluth plots, separating the dominant transverse scattering, which determines the slope, from the much smaller Coulomb scattering, determined from the extrapolated intercept. After an extensive analysis, he finds a ratio of experimental to theoretical value of the Coulomb sum rule of 0.97 ± 0.12 in ${}^{56}_{26}$Fe at $q = 570\,\mathrm{MeV/c}$.[7]

It is interesting to investigate other effects on the electromagnetic response surfaces produced by short-range correlations. Figure 23.14 shows the Coulomb response for the reaction n.m.(e, e′ N) on a nuclear matter (n.m.) Fermi gas with hard-core interactions [Fe71]. The figure is from

[7] The extensive set of current experimental data on separated longitudinal and transverse quasielastic response surfaces for ${}^{40}_{20}$Ca is discussed in [Wi97].

https://doi.org/10.1017/9781009290616.028 Published online by Cambridge University Press

Taber deForest's thesis [de66a] — done over 30 years ago in connection with the proposed program for the SCA at HEPL. The quantities $(\mathbf{q}^2, \omega)$ are arranged to be outside the allowed region for quasielastic scattering for the Fermi gas — see above and [Fe71]; thus the process can only proceed while two nucleons are in virtual collision in the nucleus.[8] The calculation of the response is *exact* to order $(k_F a)^2$ (all graphs creating 2p–2h states are retained). In Fig. 23.14 the z-axis lies along $\mathbf{q}$. While the resulting proton distribution may not look so dramatic, the backward peaking of the neutrons in the n.m.$(\mathrm{e}, \mathrm{e}' \mathrm{n})$ Coulomb response is quite spectacular.

[8] For quasielastic scattering, the indicated energy conservation region would have to intersect the Fermi sphere; thus these results lie on the high-energy-loss side of the quasielastic peak.

https://doi.org/10.1017/9781009290616.028 Published online by Cambridge University Press